Silicon Thin Films

Reynolds, Steve; Welter, Katharina; Smirnov, Vladimir

Published in:
physica status solidi (a)

DOI:
10.1002/pssa.201800847

Publication date:
2019

Document Version
Peer reviewed version

WILEY-VCH

DOI: 10.1002/pssa.201800635
Article type: Feature Article
Title: Silicon Thin Films: Functional Materials for Energy, Healthcare and IT Applications
*Author(s), and Corresponding Author(s)**
Steve Reynolds, Katharina Welter, Vladimir Smirnov*

Dr. Steve Reynolds,
University of Dundee,
School of Science and Engineering,
Nethergate,
Dundee DD1 4HN
Scotland
E-mail: s.z.reynolds@dundee.ac.uk

Dr. Vladimir Smirnov,
IEK-5 Photovoltaik,
Forschungszentrum Jülich GmbH,
52425 Jülich,
Germany.

Ms. Katharina Welter,
IEK-5 Photovoltaik,
Forschungszentrum Jülich GmbH,
52425 Jülich,
Germany.

Author Accepted Manuscript version of Reynolds, S, Welter, K & Smirnov, V 2019, 'Silicon Thin Films: Functional Materials for Energy, Healthcare, and IT Applications' physica status solidi (a). https://doi.org/10.1002/pssa.201800847

Keywords: silicon thin films, thin film transistors, displays, solar fuels, flexible electronics

Abstract:

We review selected topics in the development of hydrogenated amorphous silicon (a-Si:H), from its emergence some fifty years ago to its present status as a mature thin-film semiconductor, with market successes including flat-panel displays, solar modules and x-ray scanners. By altering process gas mixtures and deposition conditions, films with a range of atomic, structural and amorphous/crystalline phase compositions may be deposited, offering tunable bandgap, refractive index and light-scattering properties. Films thus ‘functionalized’ have greatly increased scope and utility. Three emerging applications are reported, and more extensive sections on two topics of current importance are presented: (i) Multi-junction thin film silicon solar cells for water splitting applications; and (ii) Thin-film silicon solar cells on flexible substrates.

1. Introduction

This article was motivated by the unveiling in April 2018 of an IEEE 'Milestone' plaque[1] by IEEE President Elect, Jose Moura, recognising the contributions of the research team at the University of Dundee in the development of the amorphous silicon thin-film transistor (TFT)[2] in the 1970s and 80s (**Figures 1, 2**). The TFT is the most successful commercial application of amorphous silicon to date. As pixel addressing elements in active-matrix liquid-crystal displays, TFTs were until recently (quite literally) behind every TV and laptop screen, a worldwide market worth many billions of dollars annually.

Walter Spear[3] and Peter LeComber[4] led research on the physics and technology of amorphous semiconductors at Dundee over this period. Spear left the University of Leicester in 1967, having been appointed to the Harris Chair of Physics, and was joined in Dundee by LeComber who took up a lectureship. They began work on amorphous silicon prepared by

Figure 1. IEEE 'Milestone' plaque (Dundee, April 2018). Dr Roderick Gibson was a member of the Dundee team who developed the amorphous silicon thin-film transistor into a commercially-successful device. Rod was responsible for film growth.

glow-discharge decomposition of silane gas on to a heated substrate. This material had been shown by Chittick et al[5] to possess properties consistent with a 'good' semiconductor – large thermal activation of the dark current, marked sensitivity to impurities (doping), and strong photoconductivity. Spear and LeComber also set up characterisation facilities including field-effect and carrier transport measurement systems. They showed these films had a greatly reduced electronic defect density[6] when compared with evaporated or sputtered materials. This was later confirmed to be a result of termination of silicon dangling bonds by hydrogen present in the glow discharge, and the material became known as 'hydrogenated' amorphous silicon, or a-Si:H. Electron mobility at room temperature[7] was less than 1% of that of crystalline silicon, closer in magnitude to other amorphous semiconductors such as selenium and chalcogenide glasses. Glow-discharge, or plasma-enhanced chemical vapour deposited (PECVD) a-Si:H began to attract significant scientific and commercial interest.

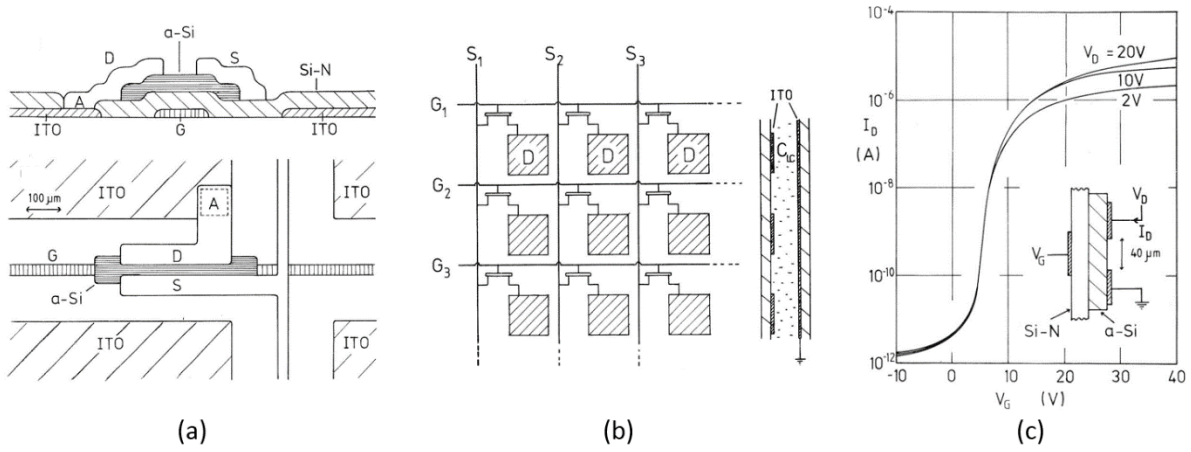

Figure 2. (a) TFT device layout; (b) TFT as switching element in matrix array; (c) transfer characteristics - drain current vs. gate voltage. Importantly, the high on : off current ratio (>10^6) is sufficient to enable both rapid charging of the selected pixel and minimal discharge until the next display refresh cycle. Reproduced with permission.[2]

Three years later, Spear and LeComber published a detailed study of n- and p-type doping in a-Si:H by addition of phosphine or diborane to the process gas[8], confirming Chittick's earlier observations and demonstrating that conductivity could be varied by some 10 orders of magnitude. Carlson and Wronski at RCA Laboratories,[9] who had been working independently on doping, announced the first a-Si:H p-i-n solar cell, a 2.6% efficient device, in 1976. Solar conversion efficiencies improved steadily, and by the mid-1980s RCA had reached 6% in the laboratory. By the turn of the century this had doubled to 12%, with United Solar holding the record. Since then, increases have been more modest, and the present 'best research cell' record is 14.0%, held by AIST.[10] This compares unfavourably with values of over 20% for competitors in bulk (wafer) silicon,[10] and CIGS and CdTe thin film technologies.[10] However, silicon is earth-abundant, whereas indium and tellurium are scarce and cadmium is highly toxic, so raw material availability and prices, and legislation, may be significant considerations in the longer-term. a-Si:H continues to dominate the consumer electronics market for scavenged power to drive calculators and novelty goods, and is a strong competitor in emerging applications such as integration into clothing and packaging.

Over the past 50 years, many academic and industrial groups worldwide have contributed to the advancement of amorphous silicon and related materials and devices (see **Figure 3** for historical examples). A compendium of hydrogenated amorphous silicon research from its beginnings up until 1990 is provided by Street's classic book[12]. The development of TFTs and amorphous and microcrystalline silicon solar cells, in both laboratory and production, is described in detail by Brotherton[13] and Shah[14], respectively.

In section 2 below, we discuss the role of amorphous silicon as a functional electronic material, whose properties may be modified to suit a range of applications by tuning the process gas and deposition conditions. A summary of successful commercial applications in

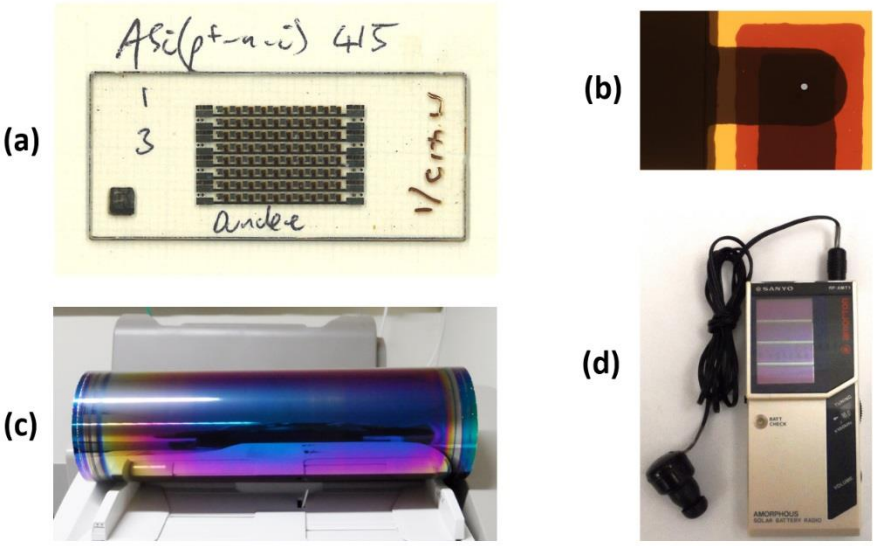

Figure 3. (a) a-Si:H p^+-n-i two-terminal non-volatile resistive memory 'pore' test cells (1986), developed by BP Research Centre and Dundee and Edinburgh Universities.[11] (b) Memory ON-state resistance was found to be independent of 'pore' top contact diameter (2 to 200 μm, highlighted by grey dot), confirming conduction is via single thin filament. (c) a-Si:H coated photocopier drum. (d) Sanyo 'Amorphous Solar Battery Radio' RP-AMT1 (1984). When sunny, four a-Si:H solar cells (top left) re-charge the NiCd battery.

addition to the TFT and a-Si:H thin-film solar cell is given in section 3, with a brief view of future trends in section 4. A selection of emerging topics having potential for commercial development is given in section 5. Sections 6 and 7 provide accounts of two areas of applied energy research currently attracting significant interest. These are: *Multi-junction thin film silicon solar cells for water splitting applications*; and *Thin-film silicon solar cells on flexible substrates.* We offer some concluding remarks and observations in section 8.

2. Amorphous silicon – an evolving functional material

The title of this paper proposes that silicon thin films are 'functional materials', which may be interpreted as 'materials whose properties derive from and are controlled by their underlying character'. Some definitions impose further requirements, that the material adapts or conforms to a given environment or stimulus, such as a piezoelectric, ferroelectric or 'smart' material. Functional materials may be viewed more broadly however, as building blocks whose properties may readily be modified for a variety of technology applications. Hydrogenated amorphous silicon fits within this definition.

The original a-Si:H material deposited by RF decomposition of silane gas onto a heated substrate performs reasonably well as an active semiconductor layer, and was utilised in this form in early solar cells, TFTs and other applications. Further, by introducing additional gases into the PECVD chamber (ammonia, methane, carbon dioxide, germane…) a range of 'alloys' (silicon nitride, silicon carbide, silicon oxide, silicon-germanium) were obtained, with optical and electronic properties[15] more suited to certain specific applications. Silicon nitride is an excellent insulator, and is employed as gate dielectric in many TFT designs. Addition of carbon widens the energy band-gap, and this material has found use as a p-type 'window' layer in a-Si:H solar cells to improve short-wavelength external quantum efficiency. Silicon (sub)oxide offers a similar advantage. Silicon-germanium is a lower-bandgap material, used as a bottom-cell absorber layer in certain multiple-junction cell designs. Thus we see that the basic material may be functionalised by adjustment of its elemental composition.

Early work revealed that the opto-electronic properties of a-Si:H films were significantly degraded on prolonged exposure to light at solar intensities. Films became less photoconductive, with a significantly lower dark conductivity, and solar cells less efficient,

with fill-factor particularly affected. Staebler and Wronski[16] were first to report in detail on what is now known as the Staebler-Wronski effect (SWE), associated with the creation of additional dangling bond (DB) defects (up to 10^{17} cm^{-3} at one sun irradiance), similar in character to the native DB defects formed on film deposition (typically 10^{15}-10^{16} cm^{-3}). The additional light-induced defect density causes the Fermi level to shift towards mid-gap (pristine a-Si:H is slightly n-type[8]), consistent with the observed reduced dark conductivity. Thermal emission from these states results in a quantitative increase in reverse dark current in solar cells, and a characteristic ESR spin signature. The SWE is however a *metastable* effect, and may be reversed by thermal annealing slightly below the substrate deposition temperature (typically 150-180 °C) for the order of an hour.

While the detailed mechanisms[17] of light-induced defect creation and annealing remain somewhat uncertain, it is known that the process is driven by recombination via the deeper band-tail states. This may disrupt weak Si-Si bonds through a process mediated by mobile hydrogen, resulting in creation of DB defects. The kinetics of formation follow a $t^{1/3}$ power-law, denoting that the creation rate is strongest at short times, with a saturated DB density proportional to $G^{2/3}$ where G is the photocarrier generation rate.

It was known (or at least surmised) from the 1970s that the limits to performance of early a-Si:H devices were constrained by high (native and SWE) deep defect density, broad band tails (shallow traps) and low carrier mobility relative to single-crystal silicon. Early commercial solar modules were strongly affected by SWE, with already low (5%-7%) conversion efficiencies reduced by one third after the first few months[18] of operation. Research addressed these issues in a variety of directions, particularly with regard to film deposition. By diluting the process gas(es) in hydrogen, and with appropriate adjustments to deposition parameters,[19] other forms of a-Si:H-like materials, such as protocrystalline[20-22] and

polymorphous[23-28] silicon can be obtained in the transition region between amorphous and microcrystalline silicon growth. These materials have, in general, different microstructure and void fraction from standard a-Si:H, which offers the possibility of reducing defect density and light induced degradation, and also tuning the energy band gap. Improvements in optoelectronic properties including increased hole mobility[28] and mobility-lifetime product[24, 25] have also been reported, associated with changes in medium-range structural order.[20, 23]

Higher levels of hydrogen dilution, in combination with further re-optimisation of deposition parameters, yields a more crystalline thin film, referred to as *microcrystalline*, or *nanocrystalline*, silicon[13]. This is a truly mixed-phase material, consisting of crystalline columns some 30 nm wide, extended in the growth direction, within an amorphous 'tissue'. These films can be doped in a similar fashion to a-Si:H. It likewise contains significant hydrogen, and is frequently abbreviated to μc-Si:H.[29] A key feature is that it exhibits negligible light-induced metastability when compared with a-Si:H. However, both a-Si:H and μc-Si:H films are sensitive to ambient conditions, which may bring about a variety of reversible and irreversible changes in material properties.[30-32]

Varying the proportion of microcrystalline to amorphous phase significantly alters its optical and electronic properties,[33] μc-Si:H films of roughly equal phase fractions being optimal for solar cell absorber layers. With an optical band-gap of 1.1 eV, compared with 1.8 eV for a-Si:H, this material is well-placed to serve as the bottom-cell absorber layer in a μc-Si:H/a-Si:H tandem cell. Such 'micromorph' solar cells[14, 33] achieve higher stabilised PV conversion efficiencies than single cells of either thin film silicon absorber material. Cell stacking may be further extended to triple and quad cells, with further improved efficiency.[34] The improved material resilience plus the ability to make use of thin a-Si:H layers which are less strongly affected by SWE, has led to reduced degradation, as low as 5% in some

cases.[35, 36] μc-Si:H possesses much higher hole mobility than a-Si:H, leading to the possibility of TFT CMOS logic circuitry.[37]

Thus we see that by careful control of deposition conditions and process gas mixture, new formulations of thin-film silicon have been developed, with improved performance over the early amorphous silicon material and an extended range of applications. These developments illustrate ability to functionalise through structural and compositional control.

a-Si:H can also be crystallised to form polysilicon films, either thermally or by laser processing. This is a very wide and important field, but lies outside the scope of this work. Chapter 7 of reference[12] contains a comprehensive discussion of laser-crystallised TFTs and their application in both passive and electro-luminescent displays

3. Current commercial products

In addition to the a-Si:H TFT and thin-film silicon solar cell/module, several additional products comprising a-Si:H films in active roles have successfully entered the market:

- *Photocopier* drums originally utilised amorphous Se as the photoreceptor, though chalcogenide and a-Si:H layers found later application. Most photocopiers and laser printers sold today use organic semiconductor receptors, as these are better adapted to modern design and manufacture. a-Si:H remains important however for extremely high throughput copying applications, as a result of its superior durability. For example, Kyocera recently (2017) announced a new a-Si:H drum yielding one million copies before requiring replacement.[38]

- *Large area a-Si:H light sensor p-i-n diode arrays* are used in medical x-ray imaging to detect visible photons emitted by an x-ray sensitive phosphor. They may be addressed using an a-Si:H TFT matrix. A number of companies have marketed x-ray scanners of this type, most recently (2018) by Varex Imaging.[39]

- *Amorphous-Crystalline silicon heterojunction* solar cells[40] employ a-Si:H in a heterojunction with a crystalline silicon absorber layer, which increases open-circuit voltage, and also as a back-surface field layer, which improves charge collection. Test cells hold the record for the highest single-junction silicon cell one-sun efficiencies, currently 26.6%.[10] The module cost per watt-peak for this technology is similar to that of conventional crystalline silicon. However, since balance-of-systems costs now exceed PV module costs, high-efficiency cells will become increasingly favoured in future.

4. Present trends

Continued small improvements in 'standard' wafer-based silicon solar module efficiency and manufacturing costs, coupled with shifts in economic climate, have resulted in falling prices for these systems over the past decade and other PV technologies have found it difficult to keep pace. Thin-film a-Si:H solar modules have now dropped out of the 'grid' power race, although CIGS and CdTe thin film modules are competitive.[41] In research labs,[10] solar cells based on organic semiconductors, quantum dots and, particularly, methylammonium lead halide perovskites show steep annual improvements in conversion efficiency, but stability and durability are proving elusive and full-scale commercial development seems unlikely in the immediate future.

In display technology, the need for devices operating beyond the physical capabilities of the a-Si:H TFT has seen its market share reduce. With the advent of OLEDs and increasing demand for large area high-quality displays, matrix switching transistors[42] need to work faster, carry higher current densities and occupy less area than hitherto. a-Si:H can no longer trade on the high on : off current ratio requirements of AMLCDs, and low carrier mobilities cannot be offset by geometric factors. Polysilicon,[43] and semiconducting oxide-based[44] TFTs which have the additional advantage of being transparent to visible light, offer mobilities 10-100 times higher than a-Si:H, which is now restricted to applications at the portable small-screen low-cost end of the market.

Organic semiconductor TFTs[45] now achieve similar levels of performance to the a-Si:H TFT. They can also be solution-processed or printed at ambient temperatures, offering significant manufacturing advantages. While there are exciting opportunities for all-plastic electronics, this technology has yet to develop strong market impact.

5. Emerging applications of thin-film silicon

While thin-film solar cell and TFT products now play a minor commercial role, emerging applications in which a-Si:H and related materials may play key roles remain buoyant. They enjoy the benefits of a mature technology, strengths and weaknesses are generally well-known, and there is an abundance of scientific and technical knowledge and expertise to call upon. A brief summary of a selection of these developments is given below:

- *Monolithic perovskite/c-Si tandem solar cells* have the potential to exceed the theoretical efficiency limit of 33% for single junctions, and could reach some 40%.

While present lab efficiencies achieved are around 20%, this challenge has attracted a great deal of attention. Significant optical losses arising at the interface between the sub-cells can be reduced by introducing a dielectric layer stack. It has been shown[46] that *doped microcrystalline silicon oxide* has excellent optoelectronic properties for this application. This material was originally developed for use in thin-film silicon solar cells, but its versatility as a functional material[47] is clear.

- A *'lab-on chip'* is a miniaturised system designed to perform bio-analysis faster and more economically than a standard laboratory, at the point of use. Petrucci et al[48] have integrated several of the functions required on to a single glass substrate, including a-Si:H diode arrays that sense both light (proportional to short-circuit current) and temperature (proportional to voltage when driven at constant dark current).

- A *non-volatile memory TFT* was fabricated by Sanjeevi et al[49] as a modification of a standard a-Si:H TFT process. A purposely defective layer was introduced during fabrication by removing a sacrificial layer of a-Si:H deposited on the gate dielectric by dry-etching. Through this defect engineering step they were able to write/erase non-volatile threshold voltage shifts through positive and negative high-voltage pulses applied to the gate. This offers the possibility of pre-storing images or other data at the display level rather than in remote electronics.

6. Multi-junction thin film silicon solar cells for water splitting applications

Hydrogen, a storable and renewable fuel, has attracted much recent interest due to an urgent need to address the problems posed by a limited supply of fossil fuels, and the negative impact of CO_2 generated by their combustion on the world climate. Currently, hydrogen is mainly produced by steam reforming of hydrocarbons from fossil fuels. A more desirable approach, which may avoid any use of fossil fuels, is via the electrolysis of water, which may be performed sustainably by photovoltaic-biased electrosynthetic devices.[50, 51] A photovoltaic (PV) cell is used as one photoelectrode in an electrochemical (EC) cell to drive the water-splitting reaction, which yields hydrogen and oxygen. The potential difference required consists of the thermodynamic potential E_{thermo} = 1.23 V, plus overpotentials occurring at the two electrodes E_{overp}. In practice this means that the PV cell must generate at least 1.5 V at the operating point, preferably accompanied by a reasonably high photocurrent since this determines the rate of hydrogen evolution.

Photovoltaic-electrochemical (PV-EC) water splitting is a topic of intense research activity, and several successful water splitting device concepts based on various types and combinations of photoelectrodes and solar cells have been reported.[52, 53] Multi-junction thin film silicon solar cells are promising candidates to fulfil the requirements of an electrical power source in light induced water splitting devices.[54, 55] They can provide a voltage suitable for driving the water splitting reactions, in the range of 1.5 – 2.8 V, by two to four sub-cells connected in series. This series stacking is achieved as a natural consequence of sequential deposition of the layers comprising the cells. Additionally, the different band gap energies of the sub-cell absorber layers enable more efficient use of the solar spectrum to be made. Furthermore, silicon is earth-abundant, and due to the thin film manufacturing approach,

material costs can be reduced. Thin film silicon solar cells are sufficiently stable under long term operation[56] for this application, and are a proven technology.

Figure 4 shows the current density-voltage curves of a range of thin film silicon multi-junction cells. The theoretical operating point of the water splitting device is indicated, at E_{thermo} = 1.23 V. For simplicity, overpotentials occurring at electrodes are not included in this illustration. These depend strongly on electrode material and lie between 300-500 mV.[59] Thus, in a real system, the voltage furnished by the PV cell at the operating point must lie in the range 1.5 – 2 V. This requirement is fulfilled for all thin film silicon based multi-junction

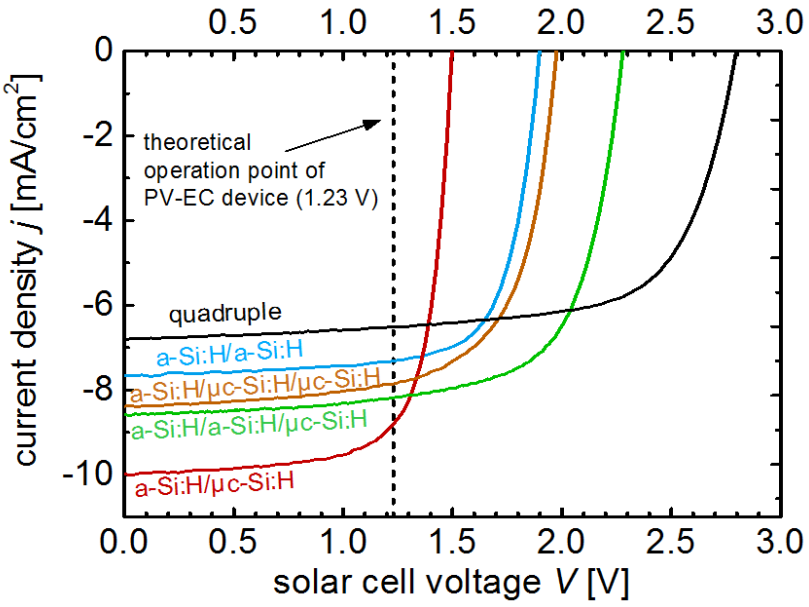

Figure 4. Current density-voltage curves for different multi-junction cells. The theoretical, ideal operation point of a light induced water splitting device is indicated at $E_{thermo.}$ = 1.23 V. Including the electrode overpotentials, the voltage at the operation point must be in the range of 1.5 – 2 V. Adapted with permission.[54, 57, 58]

cells, except for the a-Si:H/µc-Si:H tandem cell. If the a-Si:H/µc-Si:H tandem cell were to be used in a water splitting device, the electrode overpotentials would need to be close to zero.

In a multijunction solar cell, the total photocurrent generated is divided between the individual sub-cells. However, charge continuity dictates that the current in a load connected to its terminals will be limited by the lowest sub-cell photocurrent in the cell stack. Thus, the individual sub-cell currents must be carefully matched to maximize the current supplied to the electrochemical cell. **Figure 4** also shows the trade-off between photocurrent density and photovoltage. The highest short circuit photocurrent density is achieved for the a-Si:H/µc-Si:H tandem cell, which provides the lowest open circuit voltage. Whereas, the lowest short circuit photocurrent density is obtained for the quadruple junction cell (a-Si:H/a-Si:H/µc-Si:H/µc-Si:H), which at 2.8 V has the highest open circuit voltage of all multi-junction cells investigated.

To avoid failure, the solar cell must be protected against corrosion by the electrolyte, which is either strongly alkaline or acidic. This may be achieved either by depositing protective coatings or layers such as TiO_2 directly on to the back contact of the solar cell, or by bonding thin metal sheets to the back contact. A schematic setup of a PV-EC device employing an a-Si:H/a-Si:H/µc-Si:H triple junction solar cell is shown in **Figure 5**. The different sub-cells are indicated. Here, the solar cell is directly in contact with a platinum layer (either thin deposited film or metal sheet), which serves as both a hydrogen evolution reaction (HER) catalyst and as protection against the electrolyte. The counter-electrode with ruthenium oxide as

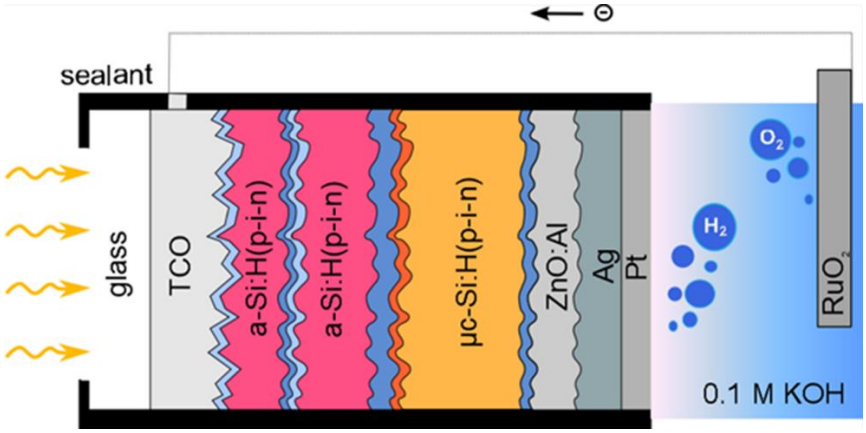

Figure 5. Schematic setup of a multi-junction based thin film silicon water splitting device. Platinum is used as hydrogen evolution reaction catalyst and additionally serves as protection against the corrosive alkaline electrolyte. Ruthenium oxide is used as counter electrode and oxygen evolution reaction catalyst. Potassium hydroxide is used as electrolyte. Adapted with permission.[57, 60]

oxygen evolution reaction (OER) catalyst is immersed in the electrolyte and electrically connected to the front contact layer of the solar cell stack (TCO). Under illumination, as shown in **Figure 4**, the photovoltage generated by the triple junction cell exceeds the voltage needed for electrolysis to commence and evolution of hydrogen and oxygen occurs at the respective electrodes, as shown in **Figure 5**. The integrated device approach shown here enables the individual optimization of the device parts (solar cell and catalyst materials), since they can be modified or adjusted independently. For example, modifications to the HER catalyst do not influence the properties and performance of the solar cell, and vice-versa. Additionally, the solar cell can be illuminated directly, since it is not immersed in the electrolyte, and thus the solar spectrum is not altered or attenuated. Using this setup with different multi-junction cells, the current density-voltage curves shown in **Figure 6** are obtained under 1 sun illumination. The operating point for unbiased water splitting is indicated at 0 V. The operating current for

each combination is represented by the intersections of the 0 V line with the appropriate current density-voltage curve. As expected from **Figure 4**, the a-Si:H/µc-Si:H tandem cell provides a low output voltage, and the operating current density J_{OP} in the water splitting reaction is very low (below 1 mA/cm^2). Tandem cells consisting of an a-Si:H/a-Si:H cell stack deliver sufficient voltage and current density for satisfactory unbiased water splitting, but even better performance (faster hydrogen evolution) is obtained with triple and quadruple junctions. With the quadruple junction (a-Si:H/a-Si:H/µc-Si:H/µc-Si:H), the threshold voltage is exceeded by some margin when using platinum and ruthenium oxide as catalysts, as shown here. Such quadruple junctions are thus of particular interest if cheaper catalyst systems with higher overpotentials, i.e. non-noble metal based materials, are to be used in the PV-EC[54] device.

The highest current densities at the operating point (V = 0 V) in 0.1 M potassium

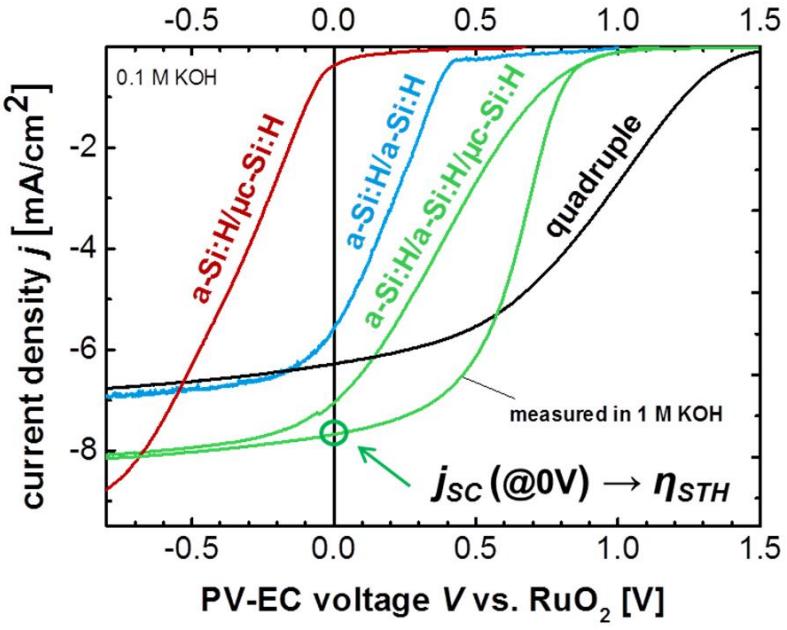

Figure 6. Current density-voltage curves for PV-EC devices employing different multi-junction cells, in 0.1 M KOH and 1 M KOH. Platinum and ruthenium oxide were used as catalysts. The operating voltage (0 V) for unbiased solar driven water splitting is indicated. Adapted with permission.[54,58]

hydroxide solution are measured for the PV-EC device based on the a-Si:H/a-Si:H/µc-Si:H triple junction cell. If the electrolyte concentration is increased to 1 M, the electrolyte conductivity also increases, reducing the voltage drop across it, and the operating current density is improved to J_{OP} = -7.7 mA/cm². J_{OP} is directly proportional to the solar-to-hydrogen (STH) conversion efficiency, which represents the amount of hydrogen produced per incident illumination power. This is calculated according to equation (1):

$$\eta_{STH} = (\Delta E \,.\, J_{OP} \,.\, \eta_F) \,/\, P_{IN} \qquad (1)$$

Here, ΔE is the thermodynamic water splitting potential, which equals 1.23 V, J_{OP} is the current density at the operating point, η_F is the Faradaic efficiency, which has been shown to equal unity, and P_{IN} is the incident illumination power (1000 W/m²). Using the above equation for the PV-EC device, the resulting STH efficiency based on the a-Si:H/a-Si:H/µc-Si:H triple junction cell in 1 M KOH, is calculated to be 9.5%.[54] To the best of our knowledge, this is the highest value reported for thin film silicon multi-junction solar cells employed in water splitting devices. Hu *et al*[61] have shown that theoretical STH efficiencies of over 25% are possible for an ideal PV-EC system driven by a tandem cell with top and bottom cell bandgaps of 1.75 and 1.15 eV respectively.

These results demonstrate the high potential for application of thin film silicon multi-junction cells in water splitting devices. STH efficiencies above 10% are achievable through the multi-junction solar cell approach, especially if catalysts that show a high performance in alkaline media are used.[59] However, for a successful commercial realization of these PV-EC devices, device upscaling beyond laboratory size (shown in **Figure 7**) must be considered. In this context, a range of challenges need to be met by the solar cell, catalysts, protection layers, device design and electrical engineering. These have recently been investigated.[62, 63] Additionally, if multi-junction based PV-EC devices are to be used outdoors, the prevailing

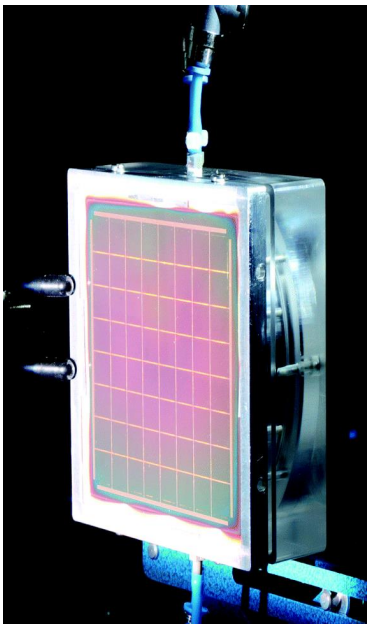

Figure 7. Photograph of the laboratory-size integrated PV-EC device[57] under illumination. The solar cell measures 8 x 8 cm.

conditions, such as temperature, intensity and spectral composition, play a major role in the device efficiency[60, 64, 65].

In summary: *Light induced water splitting, based on PV-EC devices driven by thin film silicon multi-junction solar cells is a promising sustainable low-carbon alternative for hydrogen production via electrolysis using solar energy, when compared to conventional hydrogen production from fossil fuels. Challenges in optimizing solar to hydrogen conversion remain, for example in reducing overpotentials by the development of cheap and effective catalysts. Protection from corrosion to extend device lifetime is also an important area for development. Through improvements in both solar cell and catalyst components, such PV-EC systems are anticipated to achieve STH efficiencies in excess of 10%.*

7. Thin-film silicon solar cells on flexible substrates

Thin-film technologies have potential in applications such as building integrated photovoltaic (BIPV) systems, flexible electronics and mobile power supplies.[66-69] Thin-film PV materials can be prepared on flexible substrates in a roll-to-roll manufacturing process, which offers not only a reduction in costs by high throughput production, but also opens up new markets where flexible and lightweight products are required. These PV systems can be integrated at low cost in existing structures and architectures such as windows and roofs, external as well as internal walls in buildings, and incorporate design elements of various shapes and sizes. Overall, the forecast for flexible photovoltaics market is estimated to be 70 billion US dollars by 2030.[70]

Among the various types of thin-film technology, thin-film silicon offers several advantages: (i) relatively low process temperatures, below 200 °C, by using plasma-enhanced chemical vapor deposition (PECVD) from the gas phase, making the preparation process compatible with a wider choice of substrates, especially low cost plastics or paper substrates; (ii) the PECVD process can readily be scaled up, enabling large area and high throughput manufacturing by roll-to-roll processing,[69, 71] (iii) particularly thin layers may be used, in conjunction with the high mechanical flexibility of thin film silicon.[72, 73]

Flexible substrates for thin film silicon PV must also fulfil several requirements:[69, 74, 75] (i) a thermal stability compatible with preparation conditions when depositing functional layers (e.g. thin film silicon, TCO), (ii) mechanical flexibility and durability and, in the case of transparent substrates, (iii) appropriate optical transmission. Various plastic substrates, such as polyethylene naphthalate (PEN), polyethylene terephthalate (PET) or polycarbonate (PC) as well as paper-based substrates are particularly attractive candidates[69, 75] for flexible thin film photovoltaics, due mainly to their light weight, high flexibility and low cost.

Despite the many advantages of flexible thin film silicon photovoltaics, implementation is not straightforward. For example, transparent polymer substrates such as PET impose a temperature limit of < 150 ˚C for all fabrication processes.[76] This requires the development of thin-film silicon layers and solar cells entirely prepared at comparatively low temperature, as well as transparent conductive oxide (TCO)[76] and associated light management schemes. This can limit the electronic quality of the functional layers, and the overall device performance.

A number of successful approaches have been introduced to meet these technological challenges. For example, thin film silicon solar cells deposited at low temperatures, compatible with flexible polymer or paper-based substrates, are particularly sensitive to, and may be significantly improved by, post-deposition thermal annealing processes. Brinza et al. investigated a-Si:H solar cells deposited at 100 °C and observed a relative efficiency increase of up to 40 % after post-deposition annealing, due mainly to an increase in V_{OC}.[77] An increase in the conversion efficiency up to a factor of 5, due to increase in the short-circuit current density, was reported for the thin film silicon solar cells deposited at 75 °C and annealed at 110 °C.[78] Recently, Wilken et al[79] investigated amorphous thin film silicon solar cells deposited at 120 °C on both glass and flexible PET substrates, and observed significant improvement upon annealing, with increase in the relative efficiency of up to 34 %. By comparing the performance of p- and n-side illuminated solar cells, it was concluded that increased minority carrier (hole) collection is mostly responsible for the improvement in conversion efficiency following thermal annealing. It was also deduced that both the built-in field and the electronic quality of the absorber layer, particularly the mobility-lifetime products, are improved by the thermal treatment procedure.

Light management in flexible solar cells is another challenge. Conventional light management strategies[80, 81] to optimize the light paths inside the absorber and thus to increase

the device performance, cannot be used directly in the case of flexible polymer or paper substrates. For example, optimal light scattering textures of TCO layers are obtained in materials prepared at up to 500 °C.[80, 81] Such high preparation temperatures are incompatible with polymer substrates, therefore the challenge is to combine low temperature flexible substrates with existing high temperature TCO textures. This can be achieved by utilizing a nanoimprint process, which is fully compatible with both polymer and paper flexible substrates.[76, 82, 83] **Figure 8** shows the SEM images of the glass and flexible PET substrates covered by ZnO:Al with nanoimprinted textures. **Figures 8**(a)**, 8**(b) show the images of the non-imprinted glass and PET substrates, respectively, indicating similar homogeneous surfaces with small grains originating from the low temperature ZnO:Al growth. The imprint-textured glass and PET substrates, shown in **Figures 8**(c)**, 8**(d) respectively, demonstrate that the original morphology of a well-optimized high temperature ZnO:Al layer shown in **Figure 8**(e) is well replicated on both glass and PET substrates by the nanoimprint process, which results in improved light scattering properties of these substrates.[83]

Figure 9 compares the external quantum efficiencies of amorphous silicon solar cells prepared on flexible PET and glass substrates with nanoimprinted textures shown in **Figure 8**. This demonstrates that the applied nanoimprint process significantly improves the EQE curves over the entire wavelength range, confirming successful implementation of the light scattering scheme in the solar cell. Note that the increase in the EQE curves in the short wavelength range is consistent with improvement in light in-coupling to the solar cell by the imprinted texture.

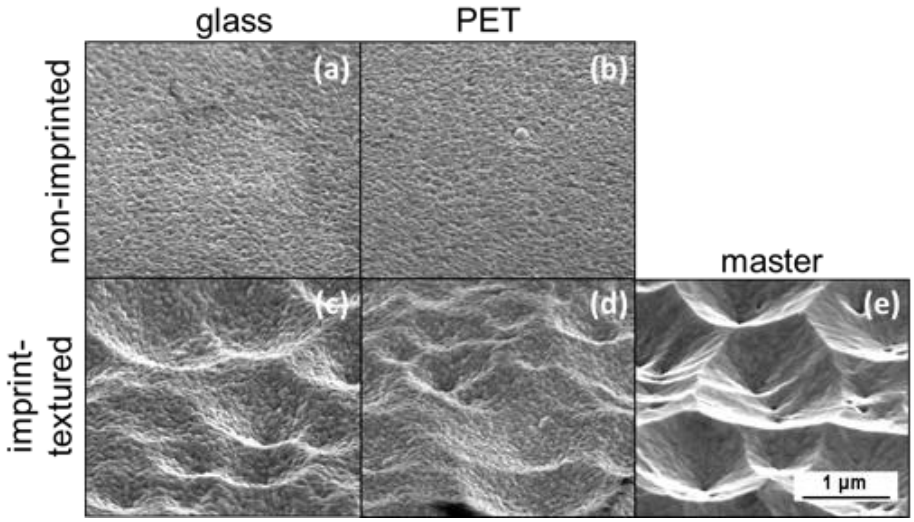

Figure 8. Scanning electron microscopy (SEM) images of the substrates covered with ZnO:Al: (a) non-imprinted glass, (b) non-imprinted PET, (c) imprint-textured glass, (d) imprint-textured PET. In (e) the master-texture of optimized high temperature ZnO:Al is shown.[83]

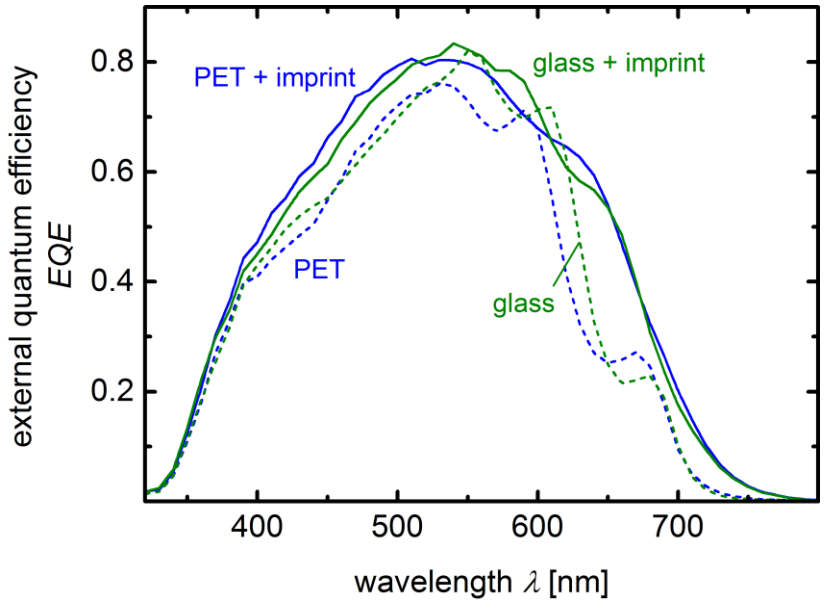

Figure 9. External quantum efficiencies of the solar cells on different substrates: non-imprinted glass (green dashed line), non-imprinted PET (blue dashed line), imprint-textured glass (green solid line) and imprint-textured PET (blue solid line).[83]

Overall, application of the nanoimprint approach enables similar EQE curves for the solar cells on flexible polymer (PET) and glass substrates to be achieved.

The nanoimprint approach can also be used successfully to maintain light management textures in the case of paper based thin film silicon solar cells.[84] As an example, **Figure 10** compares the scattering properties of the imprint- textured and bare cellulose paper substrates, demonstrating a significant improvement in the angular intensity distribution (AID) shown in **Figure 10**(a) and Haze in **Figure 10**(b) by the nanoimprint texturing. The AID curve has a maximum at a scattering angle of around 27°, similar to the angular resolved scattering (ARS) measurements reported for optimized crater-like ZnO:Al textures processed on glass substrates,[81] indicating high accuracy of the nanoimprint-based replication process of the intended surface texture on the flexible cellulose paper substrates.

A further approach to introduce light scattering features on the flexible substrates is texturing of the ZnO:Al layer by HCl vapor.[85] This method is particularly suitable for cellophane substrates, which impose further restrictions on processing temperature range and suitable solvents. **Figure 11** shows a photograph of flexible amorphous silicon thin film solar cells on ultrathin (25 μm) cellophane foils, that demonstrate superior flexibility: 90% of the initial solar cell efficiency remains after repeated bending over 50 cycles at a radius of curvature of only 1 mm.[85]

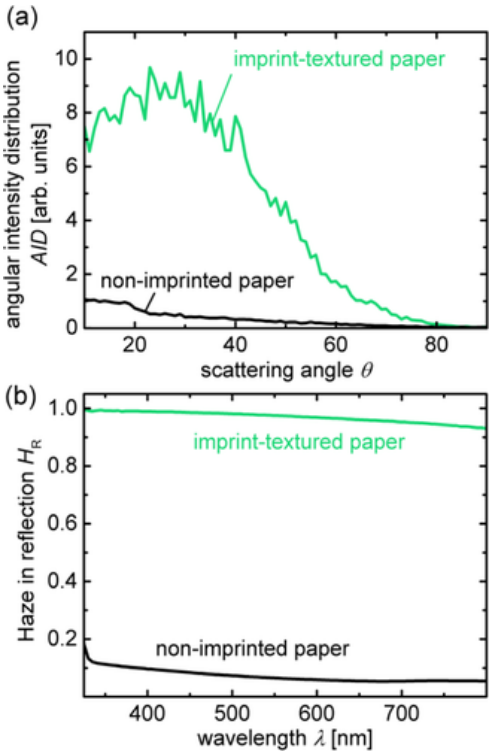

Figure 10. (a) Angular intensity distribution (AID) curves and (b) Haze in reflection (H_R) of a representative planar cellulose based substrate and imprint-textured cellulose based substrate. Adapted with permission.[84]

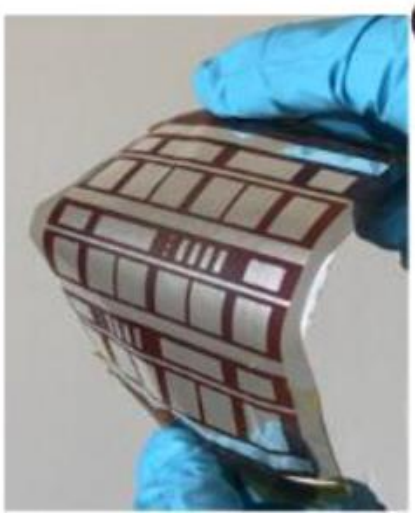

Figure 11. Photograph of flexible thin film silicon solar cells on 25 µm thick cellophane substrate.[85]

In summary: *The implementation of cheap and flexible substrates such as various plastics, cellulose and cellophane foils for thin film solar cells is a hot topic that opens a wide range of novel applications where flexibility is needed, including portable power, integration into clothing and packaging. For thin film silicon solar cells manufactured on these flexible substrates the reported efficiencies are in the range of 5-7%,[79-85] which is still lower than traditional thin film silicon solar cells manufactured on rigid glass substrates. Nevertheless, flexible thin film silicon solar cells can offer valuable advantages such as light weight, flexibility and bendability, and low cost. The challenge is to increase the efficiency further, to the level of rigid solar cells, while keeping the device highly flexible. Advanced light management concepts can assist in reducing the thickness of the functional layers, to allow even higher mechanical flexibility to be achieved.*

8. Concluding remarks

The motivation for this paper was the IEEE 'Milestone' award in April 2018 to the University of Dundee research group of the 1970s and 80s who, with important contributions from others, developed the amorphous silicon TFT to the point where it subsequently became a highly-successful commercial product.

The well-established physics of crystalline materials underpinned development of Ge and Si transistors leading the 'solid-state revolution' of the 1960s, but offered little guidance on what to expect from their amorphous counterparts – which hover mid-way between the 'bands' of the physicist and 'bonds' of the chemist. The concepts of localised and extended states, gap-state defects, correlated states, transport by hopping and multiple trapping and

substitutional doping had been introduced previously in connection with chalcogenides and disordered elemental semiconductors, but were still being developed as a-Si:H first condensed from Chittick's glow-discharge. Its birth in an industrial laboratory and nurture in the hands of academic researchers turned out to be of great interest and benefit to both parties.

Within 15 years of its discovery a-Si:H had become a material of major commercial importance, with thin-film transistors, imagers and solar cells under advanced development, and many other ideas being actively researched. The theoretical basis of film growth, carrier transport and recombination had been established, though there remained many open questions, some of which were addressed by the defect-pool model elaborated in the early 1990s. It was known and accepted that a-Si:H films had comparatively low mobilities, extensive band-tails and moderate densities of electrically-active dangling-bond gap states, and that alloys generally had poorer electrical quality. Although mechanisms are now better understood, light-induced metastability in a-Si:H remains a practical issue today, while other types of thin-film silicon, such as microcrystalline or nanocrystalline silicon, exhibit negligible effects in comparison.

It is natural (essential) for higher-performing materials to emerge to meet new needs, and to an extent, this is what has happened over the past decade in the case of the a-Si:H TFT and thin-film solar cell. As the first major thin-film active electronic material, a-Si:H was a pathfinder for these and other applications. One of us remembers, in the early 1990s, struggling to mount a new 38 kg, 28-inch CRT television on its living-room stand. In 2018 a broadly equivalent product, a 43 inch LED-backlit LCD TV, weighs 9 kg, is essentially Pb-free (several kg of Pb glass was required in a large CRT to attenuate the x-ray dose), is several times more energy-efficient and is a far superior product all round.

Although high defect densities, low mobility and metastability have been thorns in the side of a-Si:H and its extended family, resourceful scientists and engineers have, and will

continue, to circumvent these limitations and exploit the benefits of a range of thin-film silicon materials through novel design routes and positive lines of development. It seems likely that a-Si:H will play a less direct role in thin-film technology in the coming decades, while other formulations such as nanocrystalline silicon and oxide alloys with tunable optical and electronic properties will remain important materials for prototyping new devices and product concepts such as those featured above, and for supporting improvements in existing applications.

Acknowledgments

We thank R. Gibson, S. Anthony, F. Urbain and F. Finger for their advice and assistance in the preparation of this paper.

References

[1] *IEEE Milestone Plaque Marks Work of Flat Screen Innovators* (IEEE 2018). See: https://www.ieee-ukandireland.org/dundee-milestone/ (accessed October 2018).

[2] A. J. Snell, K. D. Mackenzie, W. E. Spear, P. G. LeComber, *Appl. Phys.* **1981**, *24*, 357.

[3] A. Adams, *Biogr. Mems. Fell. R. Soc.* **2009**, *55*, 267.

[4] W. E. Spear, *Biogr. Mems. Fell. R. Soc.* **1994**, *39*, 213.

[5] R. C. Chittick, J. H. Alexander, H. F. Sterling, *J. Electrochem. Soc.* **1969**, *116*, 77.

[6] P. G. LeComber, W. E. Spear, *Phys. Rev. Lett.* **1970**, *25*, 509.

[7] W. E. Spear, P. G. LeComber, *J. Non-Cryst. Solids* **1972**, *8-10*, 727.

[8] W. E. Spear, P. G. LeComber, *Solid State Commun.* **1975**, *17*, 1193.

[9] D. E. Carlson and C. R. Wronski, *Appl. Phys. Lett.* **1976**, *28*, 671.

[10] M. A. Green, Y. Hishikawa, E. D. Dunlop, D. H. Levi, J. Hohl‐Ebinger, A. W. Y. Ho-Baillie, Prog. Photovolt. Res. Appl. **2018**, *26*, 427.

[11] P. G. Lecomber, A. E. Owen, W. E. Spear, J. Hajto, A. J. Snell, W. K. Choi, M. J. Rose, S. Reynolds, *J. Non-Cryst. Solids* **1985**, *77–78*, 1373.

[12] R. A. Street, *Hydrogenated amorphous silicon*. Cambridge University Press, Cambridge UK **1991**.

[13] S. D. Brotherton, *Introduction to Thin Film Transistors : Physics and Technology of TFTs*. Springer International Publishing, Switzerland **2013**.

[14] A. V. Shah, *Thin-film Silicon Solar Cells : Photovoltaics and Large-area Electronics.* EPFL Press, Lausanne **2010.**

[15] T. Searle (ed.), *Properties of Amorphous Silicon and Its Alloys* (*EMIS Datareviews Series No. 19*). INSPEC, The Institution of Electrical Engineers, London, UK **1998**.

[16] D. L. Staebler, C R Wronski, *Appl. Phys. Lett.* **1977**, *31*, 292.

[17] H. Fritzsche, *Annu. Rev. Mater. Sci.* **2001**, *31*, 47.

[18] M. Z. Hussin, S. Shaari, A. M. Omar, Z. M. Zain, *Renew. Sustain. Energy Rev*. **2015**, *43*, 388.

[19] R. W. Collins, A. S. Ferlauto, G. M. Ferreira, C. Chen, J. Koh, R. J. Koval, Y. Lee, J. M. Pearce, C. R. Wronski, *Sol. Energy Mater Sol. Cells* **2003**, *78*, 143.

[20] R. E. I. Schropp, M. K. van Veen, C. H. M. van der Werf, D. L. Williamson, A. H. Mahan, *Mater. Res. Soc. Symp. Proc.* **2004**, *808*, A8.4.1.

[21] J. Y. Ahn, K. H. Jun, K. S. Lim, *Appl. Phys. Lett.* **2003**, *82*, 1718.

[22] Y. Ishikawa and M. B. Schubert, *Jpn. J. Appl. Phys.* **2006**, *45*, 6812.

[23] M. E. Gueunier, J. P. Kleider, *J. Appl. Phys.* **2002**, *92*, 4959.

[24] C. Longeaud, J. P. Kleider, M. Gauthier, R. Brüggemann, Y. Poissant, P. Roca i Cabarrocas, *Mat. Res. Soc. Symp. Proc.* **1999**, *557*, 501.

[25] C. Longeaud, J. P. Kleider, P. Roca i Cabarrocas, S. Hamma, R. Meaudre, and M. Meaudre, *J. Non-Cryst. Solids* **1998**, *227-230*, 96.

[26] P. Roca i Cabarrocas, A. Fontcouberta i Morral, Y. Poissant, *Thin Solid Films* **2002**, *403-404*, 39.

[27] V. Emelyanov, E. A. Konstantinova, P. A. Forsh, A. G. Kazanskii, M. V. Khenkin, N. N. Petrova, E. I. Terukov, D. A. Kirilenko, N. A. Bert, S. G. Konnikov, P. K. Kashkarov, *JETP Lett.* **2013**, *97*, 466.

[28] Y. Poissant, P. Chatterjee, P. Roca I Cabarrocas, *J. Appl. Phys.* **2003**, *94*, 7305.

[29] O. Vetterl, F. Finger, R. Carius, P. Hapke, L. Houben, O. Kluth, A. Lambertz, A. Muck, B. Rech, H. Wagner, *Sol. Energy Mater. Sol. Cells* **2000** *62* 97.

[30] V. Smirnov, S. Reynolds, F. Finger, R. Carius, C. Main, *J. Non-Cryst. Solids* **2006**, *352* 1075.

[31] S. Reynolds, V. Smirnov, F. Finger, C. Main, R. Carius, *J. Optoelectron. Adv. M.* **2005**, *7*, 91.

[32] M. Gunes, H. Cansever, G. Yilmaz, V Smirnov, F Finger, R Brüggemann, *J. Non-Cryst. Solids* **2012**, *358*, 2074.

[33] S. Reynolds, R. Carius, F. Finger, V. Smirnov, *Thin Solid Films* **2009**, *517* 6392.

[34] O. Isabella, A. H. M. Smets, M. Zeman, *Sol. Energy Mater Sol. Cells* **2014**, *129*, 82.

[35] F. Urbain, V. Smirnov, J-P. Becker, A. Lambertz, U. Rau, F. Finger, *Sol. Energy Mater. Sol. Cells* **2016**, *145*, 142.

[36] S. Kirner, S. Neubert, C. Schultz, O. Gabriel, B. Stannowski, B. Rech, R. Schlatmann, *Jpn. J. Appl. Phys.* **2015**, *54*, 08KB03.

[37] K-Y. Chan, D. Knipp, J. Kirchhoff, A. Gordijn, H. Stiebig, *Solid State Electronics* **2009**, *53*, 635.

[38] *New KYOCERA a-Si Photoreceptor Drum for Document Equipment Improves Durability, Reduces Internal Friction by 30 Percent* (Kyocera 2017) See: https://global.kyocera.com/news/2017/0308_mblf.html (accessed October 2018).

[39] *Varex Imaging:* https://www.vareximaging.com/products/medical/medical-flat-panel-detectors (accessed October 2018).

[40] W. G. J. H. M. van Sark, L. Korte, F. Roca (Eds.), *Physics and Technology of Amorphous-Crystalline Silicon Solar Cells*. Springer-Verlag, Berlin **2012**

[41] T. D. Lee, A. U. Ebong, *Renewable and Sustainable Energy Reviews* **2017**, *70*, 1286.

[42] Y. Kuo, *Electrochemical Society Interface* **2013**, *22*, 55.

[43] D. Murley, N. Young, M. Trainor, D. McCulloch, *IEEE Trans. Electron. Dev.* **2001**, *48*, 1145.

[44] E. Fortunato , P. Barquinha , R. Martins, *Adv. Mater.* **2012**, *24*, 2945.

[45] H. Klauk, *Chem. Soc. Rev.*, **2010**, *39*, 2643.

[46] K. Bittkau, T. Kirchartz, U. Rau, *Optics Express* **2018**, *26* A750.

[47] A. Richter, V. Smirnov, A. Lambertz, K. Nomoto, K. Welter, K. Ding, *Sol. Energy Mater. Sol. Cells* **2018**, *174*, 96.

[48] G. Petrucci, D. Caputo, N. Lovecchio, F. Costantini, I. Legnini, I. Bozzoni, A. Nascetti, G. deCesare, *Biosensors and Bioelectronics* **2017**, *93* 315.

[49] S. Sanjeevi, Q. Li, C-Z. Ho, W. S. Wong, *IEEE J. Electron. Devi.* **2017**, *5* 266.

[50] A. Fujishima, K. Honda, *Nature* **1972**, *238*, 37.

[51] A. C. Nielander, M. R. Shaner, K. M. Papadantonakis, S. A. Francis, N. S. Lewis, *Energy Environ. Sci.* **2015**, *8*, 16.

[52] O. Khaselev, J. A. Turner, *Science* **1998**, *280*, 425.

[53] S. Y. Reece, J. A. Hamel, K. Sung, T. D. Jarvi, A. J. Esswein, J. J. H. Pijpers, D. G. Nocera, *Science* **2011**, *334*, 645.

[54] F. Urbain, V. Smirnov, J. P. Becker, A. Lambertz, F. Yang, J. Ziegler, B. Kaiser, W. Jaegermann, U. Rau, F. Finger, *Energy Environ. Sci.* **2016**, *9*, 145.

[55] P. Bogdanoff, D. Stellmach, O. Gabriel, B. Stannowski, R. Schlatmann, R. van de Krol, S. Fiechter, *Energy Technol.* **2016**, *4*, 230.

[56] F. Urbain, V. Smirnov, J. P. Becker, A. Lambertz, U. Rau, F. Finger, *Sol. Energy Mater. Sol. Cells* **2016**, *145*, 142.

[57] F. Urbain, *Light Induced Water Splitting Using Multijunction Thin Film Silicon Solar Cells*, RWTH Aachen, **2016**.

[58] J. P. Becker, F. Urbain, V. Smirnov, U. Rau, J. Ziegler, B. Kaiser, W. Jaegermann, F. Finger, *Phys. Status Solidi Appl. Mater. Sci.* **2016**, *213*, 1738.

[59] C. C. L. McCrory, S. Jung, I. M. Ferrer, S. M. Chatman, J. C. Peters, T. F. Jaramillo, *J. Am. Chem. Soc.* **2015**, *137*, 4347.

[60] F. Urbain, J. P. Becker, V. Smirnov, J. Ziegler, F. Yang, B. Kaiser, W. Jaegermann, S.Hoch, A. Maljusch, U. Rau, F. Finger, *Mater. Sci. Semicond. Process.* **2016**, *42*, 142.

[61] S. Hu, C. Xiang, S. Haussener, A. D. Berger, N. S. Lewis, *Energy Environ. Sci.* **2013**, *6*, 2984.

[62] K. Welter, N. Hamzelui, V. Smirnov, J.-P. Becker, W. Jaegermann, F. Finger, *J. Mater. Chem. A* **2018**, 15968.

[63] J.-P. Becker, B. Turan, V. Smirnov, K. Welter, F. Urbain, J. Wolff, S. Haas, F. Finger, *J. Mater. Chem. A* **2017**, *5*, 4818.

[64] K. Welter, V. Smirnov, J.-P. Becker, P. Borowski, S. Hoch, A. Maljusch, W. Jaegermann, F. Finger, *ChemElectroChem* **2017**, *4*, 2099.

[65] V. Smirnov, K. Welter, J. P. Becker, F. Urbain, W. Jaegermann, F. Finger, *Energy Procedia* **2016**, *102*, 36.

[66] '*Technology Roadmap - Solar Photovoltaic Energy*', International Energy Agency, **2014**.

[67] A. Polman, M. Knight, E. C. Garnett, B. Ehrler, W. C. Sinke, *Science* **1972** *352*, aad 4424-1.

[68] E. Cuce, *Renewable and Sustainable Energy Reviews* **2016**, *60*, 1286.

[69] Q. Lin, H. Huang, Y. Jing, H. Fu, P. Chang, D. Li, Y. Yao, Z. Fan, *Journal of Materials Chemistry C* **2014**, *2*, 1233.

[70] '*Printed, Organic & Flexible Electronics: Forecasts, Players & Opportunities 2011-2021*', IDTechEx, **2011**.

[71] B. Yan, J. Yang, S. Guha, *Journal of Vacuum Science & Technology A* **2012,** *30*, 04D108.

[72] C. Zhang, Y. Song, M. Wang, M. Yin, X. Zhu, L. Tian, H. Wang, X. Chen, Z. Fan, L. Lu, D. Li, *Adv. Funct. Mater.* **2017**, *27*, 1604720.

[73] C. Hengst, S. Menzel, G.K. Rane, V. Smirnov, K. Wilken, B. Leszczynska, D. Fischer, N. Prager, *Materials* **2017**, *10*, 245.

[74] M. Pagliaro, R. Ciriminna, G. Palmisano, *ChemSusChem* **2008**, *1*, 880.

[75] A. T. Vicente, A. Araújo, M. J. Mendes, D. Nunes, M. J. Oliveira, O. Sanchez-Sobrado, M. P. Ferreira, H. Águas, E. Fortunato, R. Martins, *J. Mater. Chem. C* **2018**, *6*, 3143.

[76] K. Wilken, U. W. Paetzold, M. Meier, N. Prager, M. Fahland, F. Finger, V. Smirnov, *Phys. Status Solidi RRL* **2015**, *9*, 215.

[77] M. Brinza, J. K. Rath, R. E. I Schropp, *Sol. Energy Mater. Sol. Cells* **2009**, *93*, 680.

[78] C. Koch, M. Ito, M. B. Schubert, J. H. Werner, in: *16th European Photovoltaic Solar Energy Conference*, Glasgow, **2000**, p. 401.

[79] K. Wilken, F. Finger, V. Smirnov, *Energy Procedia* **2015**, *84*, 17.

[80] F. J. Haug, C. Ballif, *Energy & Environmental Science* **2015**, *8*, 824.

[81] W. Böttler, V. Smirnov, J. Hüpkes, F. Finger, *Phys. Status Solidi A* **2012**, *209*, 1144.

[82] C. H. M. van der Werf, T. M. Budel, S. Dorenkamper, D. Zhang, W. Soppe, H. R. de Neve, R. E. I. Schropp, *Phys. Status Solidi RRL* **2015**, *9*, 622.

[83] K. Wilken, U. W. Paetzold, M. Meier, N. Prager, M. Fahland, F. Finger, V. Smirnov, *IEEE Journal of Photovoltaics* **2015**, *5*, 1646.

[84] M. Smeets, K. Wilken, K. Bittkau, H. Aguas, L. Pereira, E. Fortunato, R. Martins, V. Smirnov, *Phys. Status Solidi A* **2017**, *214*, 1700070.

[85] W. Wang, V. Smirnov, H. Li, S. Moll, J. Li, F. Finger, L. Ai, W. Song, *Sol. Energy Mater. Sol. Cells* **2018**, *188*, 105.